THE JOURNAL OF BIOLOGICAL CHEMISTRY
Vol. 279, No. 10, Issue of March 5, pp. 9532–9538, 2004
Printed in U.S.A.

A Superfamily of Voltage-gated Sodium Channels in Bacteria*[S]

Received for publication, December 1, 2003, and in revised form, December 9, 2003
Published, JBC Papers in Press, December 9, 2003, DOI 10.1074/jbc.M313100200

Ryuta Koishi‡, Haoxing Xu‡, Dejian Ren§, Betsy Navarro, Benjamin W. Spiller¶, Qing Shi, and David E. Clapham‖

From the Howard Hughes Medical Institute, Department of Cardiovascular Research, Children's Hospital, and Department of Neurobiology, Harvard Medical School, Boston, Massachusetts 02115 and ¶Children's Hospital, Department of Biological Chemistry and Molecular Pharmacology, Harvard Medical School, Boston, Massachusetts 02115

NaChBac, a six-α-helical transmembrane-spanning protein cloned from *Bacillus halodurans*, is the first functionally characterized bacterial voltage-gated Na^+-selective channel (Ren, D., Navarro, B., Xu, H., Yue, L., Shi, Q., and Clapham, D. E. (2001) *Science* 294, 2372–2375). As a highly expressing ion channel protein, NaChBac is an ideal candidate for high resolution structural determination and structure-function studies. The biological role of NaChBac, however, is still unknown. In this report, another 11 structurally related bacterial proteins are described. Two of these functionally expressed as voltage-dependent Na^+ channels (Na_VPZ from *Paracoccus zeaxanthinifaciens* and Na_VSP from *Silicibacter pomeroyi*). Na_VPZ and Na_VSP share ~40% amino acid sequence identity with NaChBac. When expressed in mammalian cell lines, both Na_VPZ and Na_VSP were Na^+-selective and voltage-dependent. However, their kinetics and voltage dependence differ significantly. These single six-α-helical transmembrane-spanning subunits constitute a widely distributed superfamily (Na_VBac) of channels in bacteria, implying a fundamental prokaryotic function. The degree of sequence homology (22–54%) is optimal for future comparisons of Na_VBac structure and function of similarity and dissimilarity among Na_VBac proteins. Thus, the Na_VBac superfamily is fertile ground for crystallographic, electrophysiological, and microbiological studies.

Mammalian voltage-gated sodium (Na_V)[1] and calcium (Ca_V) channels underlie membrane excitability, muscle contraction, and hormone secretion (1). In contrast, the function of prokaryotic voltage-gated ion-selective channels is relatively unknown. Na^+ channels may drive Na^+-dependent flagellar motors in certain marine and alkaliphilic species (2–6). In marine *vibrio*, PomAB and MotXY have been proposed to form a functional Na^+ channel (5, 6), but the conductance has not been directly measured. In alkaliphilic bacteria, the prokaryotic ion channel responsible has not been identified. A bacterial 6-α-helical transmembrane (6TM) channel subunit NaChBac was expressed in CHO cells as a functional voltage-gated Na^+ channel (7), but its role in bacteria is still being elucidated.

The pore-forming subunits (α_1) of mammalian Na_V and Ca_V are composed of four similar repeats of 6TM domains (8, 9), probably arising by gene duplication of a single 6TM gene (1, 10). The first bacterial voltage-gated Na^+ channel (NaChBac) functionally expressed in mammalian cells was cloned from *Bacillus halodurans* (7). It contains a single 6TM domain of 274 amino acids but almost certainly forms a tetramer (7). NaChBac voltage-dependent activation and inactivation kinetics are 10–100 times slower than that of Na_V (7). NaChBac inactivation may result from pore inactivation (C-type inactivation), since it does not contain an obvious cytoplasmic inactivation gate (7).

Because single 6TM Na^+-selective ion channels do not appear to be present in vertebrates, the 24 TM structure of Na_Vs may have arisen under evolutionary selective pressure. It has been proposed that highly Na^+-selective Na_V channels require pore asymmetry, which is achieved by the concatenated 4 × 6TM structure (11, 12). However, tetramers of identical 6TM NaChBac are equally Na^+-selective as Na_Vs (7). Therefore, it seems more likely that the concatenated 4 × 6TM structure of vertebrate Na_Vs provided an evolutionary advantage by increasing the speed of activation, inactivation, or recovery from inactivation. To begin to address these questions, we searched for other bacterial ion channel subunits that might reveal the range of the gating speeds provided by the simplest tetrameric Na^+-selective channels. This information will also lay the groundwork for understanding their function in prokaryotes.

EXPERIMENTAL PROCEDURES

Cloning of Na_VPZ—NaChBac protein sequence (GenBank™ accession number NP_242367) was used for a BLASTP search. The nucleotide sequence of Na_VPZ was obtained from the published genomic sequence of CcaA protein of *Paracoccus zeaxanthinifaciens* (CAD24429). We synthesized DNA of Na_VPZ using the following oligonucleotides: 5′-TTACCATGGTAATGAGCCTGCGCGCGCGCCTCGACGCCCTTGTCCACGGGCGTCGTGCCCAGGGGGTGATCACCGGCGTCATCCTGTTCAA-3′ (1F), 5′-GTCCGCTGATCCTGCTGCTGGACGCGGCCTGCCTTGCCGTCTTCGTGGCCGAGATCGCGGCCAAGCTGATCGCGCGCGGCCCGCGCTTCT-3′ (2F), 5′-ATGCCGGCGGGGCAGGGCCTCTCGGTGCTGCGCGCGCTGCGCATCCTGCGTCTGCTGCGTCTGGTGTCGGTCACCCCGCGCCTGCGCCGC-3′ (3F), 5′-GCTGATGGGCGTGATCTTCTACATCTTCTCGGTCATGGCGACGAAGCTGTTCGGGGCGGGGTTCCCGGACTGGTTCGGCTCGCTTGGCAA-3′ (4F), 5′-GGATCGTGCGTCCGGTCATGCAGGAATATCCGCTGGCATGGCTGTTCTTCGTGCCGTTCATCCTGATCACGACCTTCGCGGTGATGAACC-3′ (5F), 5′-GAAAGCGCCGCCACCGACGCCTATCGCGACGAGGTGCTGATGCGCCTGCGCGCGATCGAGAAGCAGCTGGACGAAAGCGGCGGCCGTGGG-3′ (6F), 5′-CAGCAGCAGGATCAGCGGACCCGCGACCGCCATGACGCGGCCCGAGGTCTCCAGCCCCAGCAGGACGGCGTTGAACAGGATGACGCCGGT-3′ (1R),

* The costs of publication of this article were defrayed in part by the payment of page charges. This article must therefore be hereby marked "*advertisement*" in accordance with 18 U.S.C. Section 1734 solely to indicate this fact.

[S] The on-line version of this article (available at www.jbc.org) contains information on the cloning of additional NaChBac homologs.

‡ These two authors contributed equally to this work.

§ Present address: 511 Goddard Laboratories, Dept. of Biology, University of Pennsylvania, Philadelphia, PA 19104.

‖ To whom correspondence should be addressed: Howard Hughes Medical Institute, Dept. of Cardiovascular Research, Children's Hospital and Dept. of Neurobiology, Harvard Medical School, 320 Longwood Ave., Boston, MA 02115. Tel.: 617-355-6163; Fax: 617-731-0787; E-mail: dclapham@enders.tch.harvard.edu.

[1] The abbreviations used are: Na_V, voltage-gated sodium channel; Ca_V, voltage-gated calcium channel; 6TM, six-α-helical transmembrane-spanning; Na_VBac, bacterial voltage-gated sodium channel; Na_VPZ, Na_VBac from *P. zeaxanthinifaciens*; Na_VSP, Na_VBac from *S. pomeroyi*; CHO, Chinese hamster ovary.

5′-AGGCCCTGCCCCGCCGGCATCAGCGCGATGGCCACGACGCTGAAATCGAAGACGTTCCAGCCGTCGCGGAAGAAGCGCGGGCCGCGCGCG-3′ (2R), 5′-AGAAGATCACGCCCATCAGCAGGAAGACCGAGGCCATGCCCGGCATCGCGGCGAACAGCCCCTCGACCACGCGGCGCAGGCGCGGGGTGA-3′ (3R), 5′-CATGACCGGACGCACGATCCCCATCGACCAGCTTTCCAGCGTCATCACCTGGAACAGCGAATAGGCCGACTTGCCAAGCGAGCCGAACCA-3′ (4R), 5′-GCGTCGGTGGCGGCGCTTTCCTCGGCCTGGTGGGCATCCTGCATCGAGTTCACGATCAGACCGACGACAAGGTTCATCACCGCGAAGGTC-3′ (5R), and 5′-TTACTCGAGAGAACCGCGTGGCACCAGGACACGCCCACGGCCGCCGCTTTCGT-3′ (6R).

After mixing 1 μM each of 2F, 3F, 1R, and 2R as a template, the first PCR was conducted using 1F and 3R as primers (10 μM each). Similarly, 4R, 5F, 5R, and 6F were mixed, and PCR was conducted using 4F and 6R as primers. These PCR products were excised from agarose gels. Purified fragments were mixed and used as templates for further PCR, using 1F and 6R as primers. The amplified fragment was digested with NcoI and XhoI and purified from an agarose gel. The PCR product was then cloned into pTrcHis2B (Invitrogen). This synthesized DNA contained additional methionine and valine codons prior to the first methionine as required by the cloning strategy. We also intentionally introduced 10 silent mutations (45G→T, 321G→T, 330G→T, 564C→G, 606C→G, 624A→C, 775A→C, 777G→T, and 783G→T) into the synthetic DNA. An additional silent mutation (495T→C) occurred during the PCR process. Finally, this plasmid DNA was digested with SalI and XhoI and then self-ligated after the linker sequence was deleted. The resultant expression clone was used to transform *Escherichia coli* BL-21 (Stratagene).

Na_VPZ was cloned into a modified pTracer-CMV2 vector (Invitrogen) containing enhanced green fluorescent protein for expression in mammalian cells. Briefly, DNA was amplified by PCR from the *E. coli* expression clone using the following primers: 5′-AATGGATCCATGAGCCTGCGCGCGCGC-3′ (containing a BamHI site) and 5′-ATTGAATTCTCAGACACGCCCACGGCCGCC-3′ (containing an EcoRI site). The PCR product was then cloned into the modified pTracer-CMV2 plasmid (Invitrogen) between the single restriction sites for BamHI and EcoRI. All clones were confirmed by DNA sequencing.

Cloning of Na_VSP—The NaChBac DNA sequence (NC_002570) was used for a TBLASTX search against the Microbial Genomic data base at NCBI. A sample of *Silicibacter pomeroyi* was obtained from the American Type Culture Collection (catalog no. 700808). *S. pomeroyi* genomic DNA was collected by standard procedures (13). The genomic sequence homologous to NaChBac was identified, and the preliminary sequence data was obtained from The Institute for Genomic Research (TIGR) site on the World Wide Web at www.tigr.org.

Na_VSP was cloned into a pTrcHis2A (Invitrogen) for expression in *E. coli*. Briefly, DNA was amplified by PCR from a *S. pomeroyi* genomic DNA using the following primers: 5′-AATCCATGGTAATGCAAAGAATGCAGGCCTTT-3′ (containing an NcoI site) and 5′-ATTCTCGAGAGAACCGCGTGGCACCAGCTTTTTGGTTTCACCAAG-3′ (containing a thrombin recognition site and an XhoI site). The PCR product was cloned into the pTrcHis2A plasmid using NcoI and XhoI sites. This cloned DNA contains additional methionine and valine codons prior to the first methionine as required by the cloning strategy. The resulting expression clone was used to transform *E. coli* BL-21.

Na_VSP was cloned into a modified pTracer-CMV2 vector containing enhanced green fluorescent protein for expression in mammalian cells. Briefly, DNA was amplified by PCR from a *S. pomeroyi* genomic DNA using the following primers: 5′-AATGGATCCATGCAAAGAATGCAGGCCTTT-3′ (containing a BamHI site) and 5′-ATTGAATTCTCACTTTTTGGTTTCACCAAG-3′ (containing an EcoRI site). The PCR product was cloned into the modified pTracer-CMV2 plasmid between the single restriction sites for BamHI and EcoRI. All clones were confirmed by DNA sequencing. Information related to the cloning of other NaChBac homologs is provided as supplementary data.

Expression and Purification of Recombinant Proteins—100–300 ml of LB medium containing ampicillin (50 μg/ml) was inoculated from glycerol stocks and grown overnight at 30 °C. 40 ml of culture medium was inoculated into 2 liters of Terrific Broth medium (Invitrogen) containing ampicillin and grown at 37 °C to A_{600} = 1.2. Cells were induced with 1 mM 1-β-D-thiogalactopyranoside and grown at 37 °C for 3h. Cells were then suspended in PBS buffer (pH 8.0) containing protease inhibitors (Protease Inhibitor Mixture; Sigma) and lysed by sonication. The carboxyl-terminal histidine-tagged protein was extracted by homogenization and solubilization in 15 mM *n*-undecyl-β-D-thiomaltopyranoside (Anatrace). Following centrifugation, the supernatant was loaded onto a Talon Co^{2+} affinity column (Clontech). Resin was washed with 20 mM imidazole, and the protein was then eluted in the presence of 400 mM imidazole. Purified protein was resolved by 4–12% SDS-PAGE (Invitrogen) and stained with Coomassie Blue. Molecular weight marker was purchased from Invitrogen (BenchMark™ Prestained Protein Ladder).

Mammalian Electrophysiology—Na_VPZ and Na_VSP as well as other NaChBac homologues were subcloned into an enhanced green fluorescence protein-containing pTracer-CMV2 vector (Invitrogen) for expression into CHO-K1 and HEK293T cells. CHO-K1 and HEK293T cells were grown in Dulbecco's modified Eagle's medium (Invitrogen) supplemented with 10% fetal bovine serum at 37 °C under 5% CO_2. DNA was transfected using LipofectAMINE™ 2000 (Invitrogen) and plated onto coverslips, and recordings were made after 12 h (Na_VPZ) or 48h (Na_VSP), respectively. Unless otherwise stated, the pipette solution contained 147 mM Cs^+, 120 mM methane sulfonate, 8 mM NaCl, 10 mM EGTA, 2 mM Mg-ATP, and 20 mM HEPES (pH 7.4). Bath solution contained 140 mM NaCl, 2 mM $CaCl_2$, 1 mM $MgCl_2$, 5 mM KCl, 20 mM HEPES (pH 7.4), and 10 mM glucose. All experiments were conducted at 22 ± 2 °C. Unless otherwise indicated, all chemicals were dissolved in water. Nifedipine (dissolved in Me_2SO) was purchased from Sigma. As reported previously (7), unknown agents, presumably leached from the perfusion tubing, caused fast inactivation, and these perfusion systems were subsequently avoided.

RESULTS

Using the whole or partial sequence of NaChBac as the query, we performed standard BLASTP or TBLASTX searches on the GenBank™ data bases from various prokaryotic genomic sequencing projects. Several open reading frames with significant sequence homology (22–54%) to NaChBac were identified in the following species (Fig. 1*A*): *Vibrio vulnificus* (22%), *Microbulbifer degradans* (two genes, 32 and 33%, respectively), *Colwellia psychrerythraea* (two genes, 35 and 38%, respectively), *Magnetococcus* sp. (32%), *S. pomeroyi* (39%), *P. zeaxanthinifaciens* (39%), *Hyphomonas neptunium* (33%), *Thermobifida fusca* (30%), and *Oceanobacillus iheyensis* (54%). Among these species, *V. vulnificus* (14), *M. degradans* (15), *C. psychrerythraea* (16), *Magnetococcus* sp. (17), *S. pomeroyi* (18), *P. zeaxanthinifaciens* (19), and *H. neptunium* (20) were isolated from sea water or water. *T. fusca* (21), a thermophilic Gram-positive bacteria, was isolated from soil but grows optimally in alkaliphilic conditions. *O. iheyensis* (22) and *B. halodurans* (23) are alkaliphilic Gram-positive bacteria isolated from deep sea water. Based on the degree of sequence homology, we consider these proteins to be NaChBac homologs (rather than orthologs). Hydrophobicity analysis of these proteins predicted that all have the 6TM architecture. Importantly, threonine, glutamate, and tryptophan residues are conserved in the pore region in all proteins (Fig. 1*B*). These residues have been shown to be critical for the cationic selectivity of NaChBac (24). As is characteristic for voltage-gated channels (25), positively charged amino acids (Arg) are interspersed every 3 amino acids in the fourth putative transmembrane region (*S4*) (Fig. 1*C*). In *V. vulnificus* M06, however, the third arginine was not conserved. Based on the sequence homology and the structural similarity to NaChBac, it is likely that these proteins function as voltage-gated channels.

We cloned all 11 sequences (see "Experimental Procedures") and studied them by expression in mammalian cell lines. As shown below, we were able to measure currents produced by two NaChBac homologs, Na_VPZ (Fig. 2*A*) from *P. zeaxanthinifaciens* (a zeaxanthin-producing marine bacteria (19)) and Na_VSP (Fig. 2*A*) from *S. pomeroyi* (a dimethylsulfoniopropionate-degrading marine bacteria (18)). Isolation and sequencing of the gene encoding Na_VPZ revealed an open reading frame of 262 amino acids with a predicted molecular size of 29 kDa. Similarly, the Na_VSP gene encoded an open reading frame of 258 amino acids with a predicted molecular mass of 29 kDa. Na_VPZ and Na_VSP share 39% identity (60% similarity) and 39% identity (59% similarity) with NaChBac, respectively (Fig. 2*B*). Notably, Na_VPZ is 65% identical (77% similar) to Na_VSP. Upon electrophoresis, both Na_VPZ and Na_VSP proteins

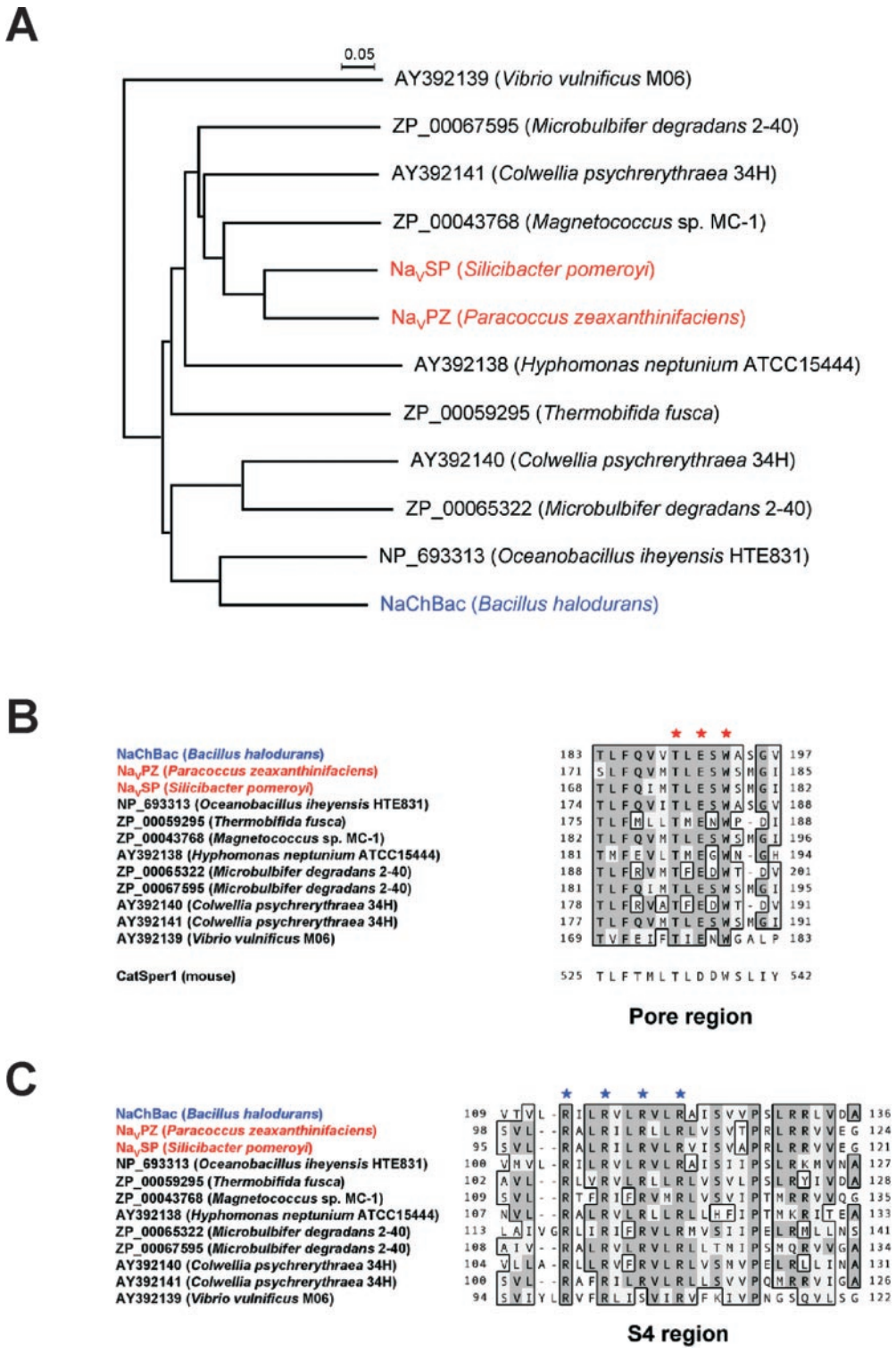

FIG. 1. **NaChBac homologs in bacteria.** *A*, phylogenic tree of bacterial NaChBac homologs. A multiple alignment of NaChBac homologs was calculated using the ClustalW program based on their conserved sequences. The tree was then generated using the neighbor-joining method (Njplot) (37). Branch lengths are proportional to the sequence divergence and can be measured relative to the *bar* shown (*top*, *bar* = 0.05 substitution per amino acid site). GenBank™ accession numbers are as follows: *V. vulnificus* M06, AY392139; *M. degradans* 2–40, ZP_00067595 and ZP_00065322; *C. psychrerythraea* 34H, AY392140 and AY392141; *Magnetococcus* sp. MC-1, ZP_00043768; Na_VPZ (*P. zeaxanthinifaciens*), CAD24429; Na_VSP (*S. pomeroyi*), AY392137; *H. neptunium* ATCC15444, AY392138; *T. fusca*, ZP_00059295; *O. iheyensis* HTE831, NP_693313; and NaChBac (*B. halodurans*), NP_242367. *B*, alignment of the putative pore regions of prokaryotic channel subunits. *C*, alignment of the putative voltage-sensing S4 region of NaChBac homologs. *Star*, conserved residues.

migrated as a single band (~31 kDa; Fig. 2*C*), almost identical to the predicted molecular sizes of the His-tagged constructs.

CHO-K1 or HEK293T cell lines were transfected with NaChBac homologs (in pTracer), and whole-cell currents were recorded 12–48 h after transfection (see "Experimental Procedures"). Among 11 NaChBac homologs, only two (Na_VPZ and Na_VSP) produced detectable currents. Similar current are not present in nontransfected or mock-transfected cells (data not shown). Na_VPZ-transfected cells exhibited large (up to 10,000 pA; 10 nA) voltage-activated inward currents (Fig. 3, *A–C*).

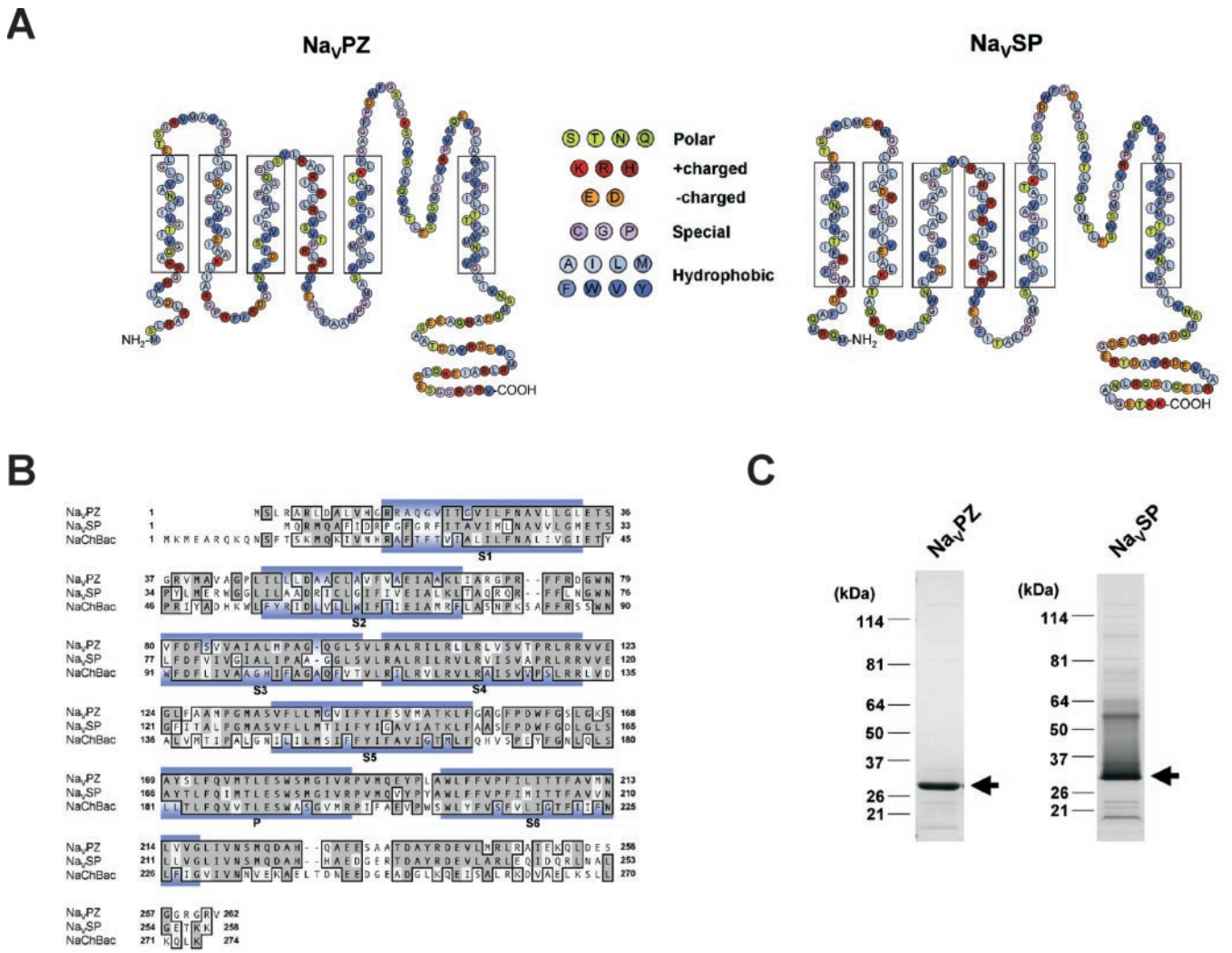

FIG. 2. **Putative primary structure of Na_VPZ and Na_VSP.** *A*, deduced membrane topology of Na_VPZ (*left*) and Na_VSP (*right*). *B*, alignment of the deduced amino acid sequence of Na_VPZ, Na_VSP, and NaChBac. The putative 6TM domains (*S1–S6*) and pore region (*P*) are indicated. *C*, Coomassie-stained SDS-PAGE of Co^{2+} affinity chromatography purification of Na_VPZ and Na_VSP, indicating that both are ~29-kDa monomers.

Na_VPZ-mediated current (I_{Na_VPZ}) activated with a time constant ($\tau_{activation}$) of 21.5 ± 1.3 ms at +10 mV (n = 19), significantly slower than both mammalian Na_V channels ($\tau_{activation} < 2$ ms) and $I_{NaChBac}$ ($\tau_{activation} < 13$ ms). Inactivation of I_{Na_VPZ} was slow ($\tau_{inactivation}$ = 102 ± 4.2 ms at +10 mV, n = 19) compared with the typically fast inactivating Na_V currents ($\tau_{inactivation} <$ 10 ms) but faster than $I_{NaChBac}$ ($\tau_{inactivation} > 160$ ms).

Cation replacement by *N*-methyl-D-glucamine NMDG (bath) resulted in complete removal of voltage-dependent I_{Na_VPZ} inward current (Fig. 3*C*). Similarly, no significant inward current was seen in isotonic $[Ca^{2+}]_o$ (monovalent cations replaced with 105 mM Ca^{2+}) (Fig. 3, *B* and *C*). I_{Na_VPZ} reversed at +75 mV (Fig. 3*C*), close to the Nernst potential of Na^+ under our recording conditions (E_{Na} = +72 mV). These results, together with the large leftward shift of the reversal by external Na^+ removal (*N*-methyl-D-glucamine$^+$ and isotonic Ca^{2+} solution substitution), suggested that Na_VPZ, like NaChBac, is a Na^+-selective channel. We assumed that the outward currents in 0 mM $[Na^+]_o$ (Fig. 3*B*) were carried by internal Na^+ (8 mM $[Na^+]_i$). Due to the very negative E_{rev} (Fig. 3*C*), sizable outward currents were observed at most voltages tested (Fig. 3, *B* and *C*).

We evaluated the voltage-dependent activation of I_{Na_VPZ} by measuring deactivation tail currents (Fig. 4*A*). A Boltzmann fit of the averaged activation curve yielded a $V_{1/2}$ of −9.5 ± 0.8 mV (n = 9) and slope factor (κ) of 10.7 ± 0.7 mV per *e*-fold change in current (Fig. 4*C*). Steady-state inactivation of the channel was determined by sequential depolarization to test voltages followed by voltage clamp to the peak of activation at +10 mV (Fig. 4*B*). Steady-state inactivation was a steep function of voltage, with 50% inactivation at −35 ± 0.4 mV (n = 10) and slope factor (κ) of 6.3 ± 0.3 mV/*e*-fold (Fig. 4*C*). We investigated the time course of I_{Na_VPZ} inactivation at −30 mV, where activation was minimal. The degree and speed of inactivation was strongly dependent on the duration of the inactivating prepulse (−30 mV; τ = 2123 ± 434 ms; n = 6; Fig. 4, *D* and *E*). I_{Na_VPZ} recovered slowly with time constant, τ = 839 ± 90 ms (n = 7, HP = −90 mV, Fig. 4, *F* and *G*).

Na_VSP-transfected cells also yielded voltage-activated inward currents (Fig. 5*A*), peaking at ~+30 mV. The E_{rev} of Na_VSP-mediated current (I_{Na_VSP}) was +76 mV. Ion substitution (Ca^{2+} replacement) experiments confirmed that Na_VSP, like Na_VPZ, was also a Na^+ -selective channel (data not shown). I_{Na_VSP} activated and inactivated significantly faster than I_{Na_VPZ} and $I_{NaChBac}$ ($\tau_{activation}$ = 3.4 ± 0.3 ms at +30 mV, n = 17; $\tau_{inactivation}$ = 35 ± 1.5 ms at +30 mV, n = 17) but still severalfold slower than Na_V currents. The Boltzmann fit activation curve yielded a V of +21 ± 0.4 mV and κ of 11.8 ± 0.4 mV/*e*-fold change (n = 28; Fig. 5*E*). Steady state inactivation was strongly dependent on the voltage (κ = 10.3 ± 0.5 mV/*e*-fold), with half-inactivation at −22 ± 0.8 mV (n = 11; Fig. 5*E*).

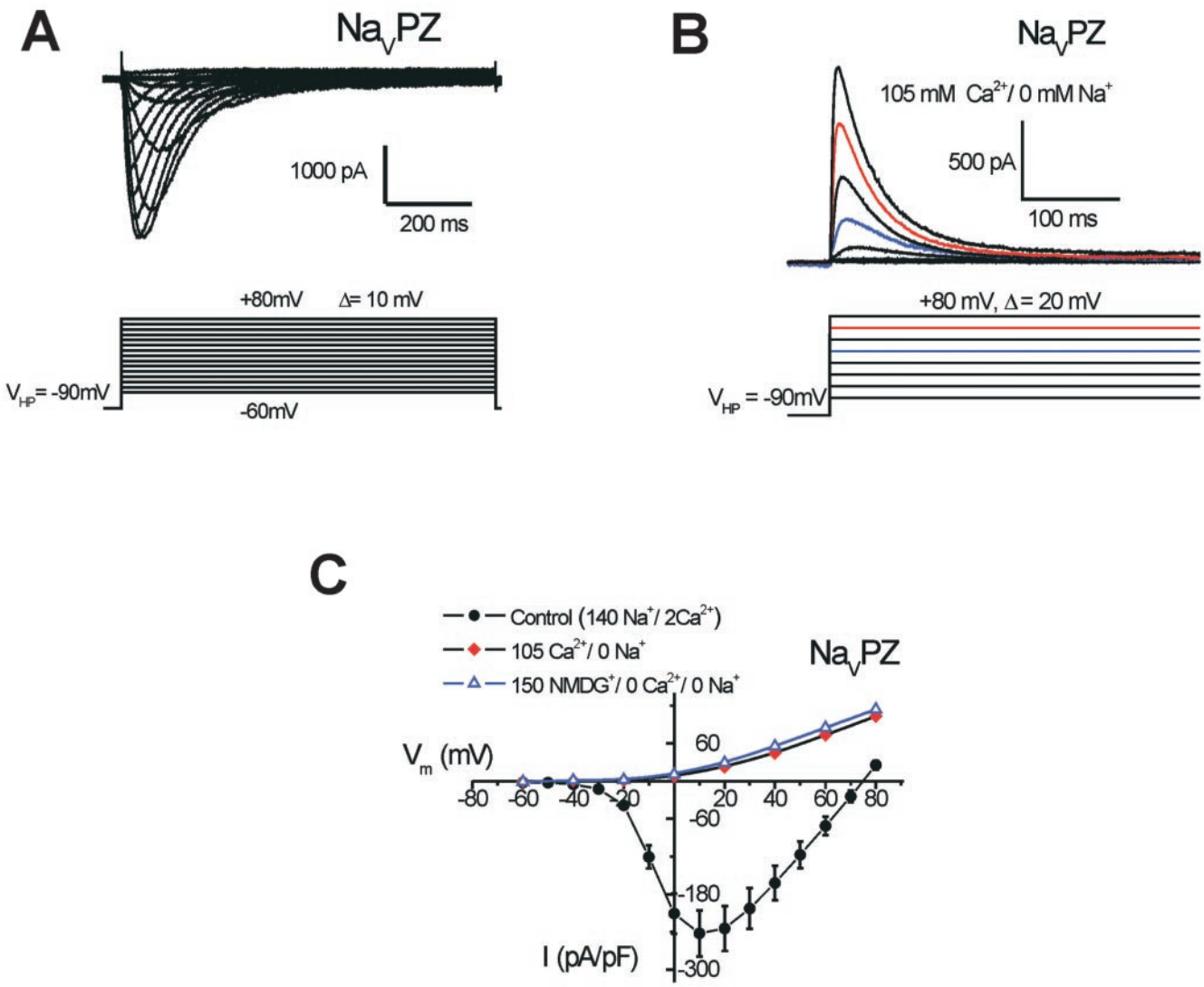

FIG. 3. **Functional expression of Na_VPZ in CHO-K1 cells.** *A*, representative traces (*top*) of I_{Na_VPZ} activated by the voltage protocol shown. The cell was bathed in 2 mM Ca^{2+} Tyrode's external solution (140 mM Na^+, 2 mM Ca^{2+}, 5 mM K^+, 1 mM Mg^{2+}, pipette; 147 mM Cs^+, 8 mM Na^+; see "Experimental Procedures"). *B*, I_{Na_VPZ} in isotonic Ca^{2+} (105 mM Ca^{2+}, 0 mM Na^+) external solution (+20 mV, *blue*; +60 mV, *red*). *C*, averaged (n = 24) peak current-voltage (*I*/V) relation of Na_VPZ in Tyrode's solution, normalized by cell capacitance (pF). E_{rev} = +75 mV. Also shown are peak current *I*-V relations of I_{Na_VPZ} from a cell bathed in either isotonic 105 mM Ca^{2+} (*diamonds*) or 150 mM *N*-methyl-D-glucamine$^+$ (0 mM Ca^{2+} (*NMDG*$^+$), 0 mM Na^+; *triangles*). E_{rev} ~−40 mV. V_{HP} indicates holding potential, 15 s between pulses.

Na_VPZ and Na_VSP were sensitive to high concentrations of nifedipine (30 μM; data not shown).

DISCUSSION

Expression of bacterial genes in systems where the protein can be studied (mammalian cells for patch clamp) is crucial to interpreting and extending static structural data through structure-function studies. Such functional expression is also important to understanding their native roles in bacteria. However, successful functional expression of bacterial proteins in mammalian cells is rare. Here, we identified 11 putative 6TM Na^+ prokaryotic channel subunit genes and were able to functionally express 2 of the 11 in mammalian cells, where their electrophysiological properties could be studied. Both channels were Na^+-selective and activated by voltage. One conclusion based on comparison of bacterial channels and Na_Vs is that the major evolutionary pressure for gene duplication and concatenation of subunits was to increase the speed of channel gating. Given the high selectivity of presumed homomeric bacterial Na^+ channels, the case for pore asymmetry as a means to increase Na^+ selectivity seems a less likely scenario.

Little is known about the molecular determinants that control mammalian Na_V activation rates. Mammalian Na_V channels activate and inactivate within a few milliseconds (<10 ms), roughly 10–100 times faster than NaChBac, the only bacterial voltage-gated channel functionally expressed up to now. Interestingly, Na_VSP activation is ~4-fold faster than NaChBac, whereas Na_VPZ activation is ~2 times slower than NaChBac, despite 77% sequence homology between Na_VSP and Na_VPZ. In Na_VSP, Na_VPZ, and NaChBac, the S4 domain and short S3-S4 linker are highly conserved, suggesting that the structural determinants for the kinetics differences are located elsewhere. Notably, there are several Na_VSP-specific residues in the putative pore-forming domains (Gly^{143} in S5, Ile^{172} in the pore loop, Val^{189} in the linker between the P loop and S6, and Met^{202} in S6). These residues may contribute to the relatively fast activation kinetics of Na_VSP.

Na^+ channel inactivation mechanisms are better understood than those of activation. Interdomain linkers mediate fast inactivation in Na_Vs by "ball and chain" or N type inactivation (26), but these domains are obviously missing in tetramers of

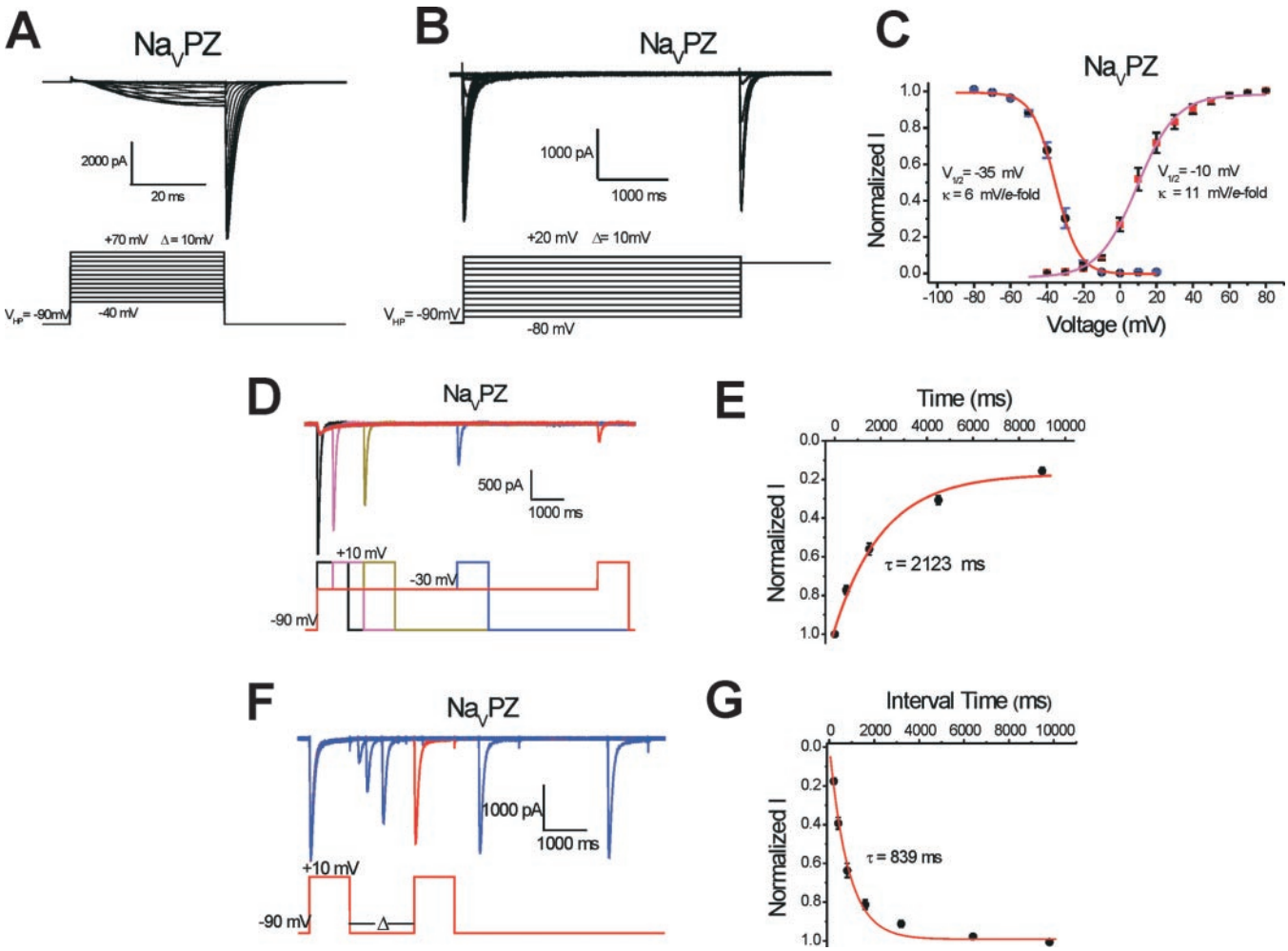

FIG. 4. **I_{Na_VPZ} voltage- and time-dependent activation and inactivation.** *A*, I_{Na_VPZ} deactivation tail currents. After prepulses of varying depolarization (from −40 to +70 mV, increments = +10 mV), tail currents were measured upon return to the holding potential (V_{HP}, −90 mV). *B*, I_{Na_VPZ} steady-state inactivation currents. After a 4-s prepulse, the currents inactivated to a steady-state level and were reactivated by a second 2-s depolarizing pulse. The intersweep interval was 16 s. *C*, normalized activation curve (n = 9; ±S.E.) and steady-state inactivation curve (n = 10; ±S.E.). *D*, time-dependent inactivation of I_{Na_VPZ} increased slowly at −30 mV. V_{HP} = −90 mV. The currents were elicited by depolarization to +10 mV preceded by a prepulse (−30 mV) with a variable length of time (0 ms (*black*), 500 ms (*magenta*), 1500 ms (*dark yellow*), 4500 ms (*blue*), 9000 ms (*red*)). *E*, the average time course of I_{Na_VPZ} inactivation at −30 mV. The time constant of inactivation development is ~2 s (−30 mV). *F*, recovery from inactivation. The time interval between the test pulse (+10 mV, 1000 s) and the inactivation pulse (+10 mV, 1000 ms) was varied from 0.2 to 9.8 s. *G*, relative peak I_{Na_VPZ} recovered with an approximately exponential time course (τ ~840 ms). The ratios between currents elicited by the two pulses (*F*) were used to construct the recovery curve (n = 7; ±S.E.).

6TM bacterial channels. Additionally, the removal of segments within the N and C cytoplasmic domains of NaChBac (24) (unpublished data) does not substantially alter its inactivation rate. If the cytoplasmic domains do not participate in inactivation, we can then begin to look at other domains. Studies on 6TM HERG K^+ channels indicated that the S5-P linker was crucial for its C-type inactivation, probably by providing allosteric coupling between its outer mouth and the voltage sensor (27). NaChBac inactivates with a time constant similar to Na$_V$PZ, but the NaChBac S5-P linker (from Gln^{167} to Ser^{180}) has low homology to Na$_V$PZ. NaChBac and Na$_V$PZ inactivates 5-fold more slowly than Na$_V$SP. In the pore-S6 linker, Na$_V$SP lacks the negatively charged glutamate present in both NaChBac and Na$_V$PZ. Future studies will focus on this and other sequence differences. However, the difficulty of obtaining functional expression of many mutants highlights the need for structural data. By exclusion of alternative mechanisms, we hypothesize that C-type inactivation, in which the Na^+ pore is shut, is the more likely mechanism for Na$_V$Bac channel inactivation.

Na^+ channels have been proposed to play a central role in Na^+-dependent flagellar mobility in some prokaryotes. Marine *Vibrio* species utilize their Na^+-driven polar flagella for swimming (5, 6), and in the alkaliphilic *Bacillus* species, $[Na^+]_o$ determines the activity of the flagellar motor (4, 28). Under alkaliphilic conditions, the H^+-motive force is weak due to the high intracellular pH (pH 8–9) of these bacteria (4, 29). Therefore, a Na^+ cycle driven by the Na^+ channel may have evolved to power the flagellar motor (4, 28, 30–32). Interestingly, bacteria whose flagellar motors are powered by Na^+ (as opposed to H^+) express NaChBac homologs. In bacteria, the Na^+/H^+ exchanger prevents cytotoxic Na^+ accumulation and also supports pH homeostasis at elevated pH (4, 31, 33). In low $[Na^+]_o$ environments or in the absence of solutes to support Na^+ uptake through Na^+-coupled solute transporters, the pH homeostasis function may rely on a Na^+ channel (4, 31, 33). We propose that sustained voltage-gated Na^+ channel opening is primarily responsible for this Na^+ entry (33). It is possible that some mammalian Na^+ channels play a role in Na^+ or H^+ homeostasis. Interestingly, the mammalian persistent and resurgent Na^+ currents have similar kinetics to Na$_V$Bac (34, 35). These persistent Na^+ currents may be mediated

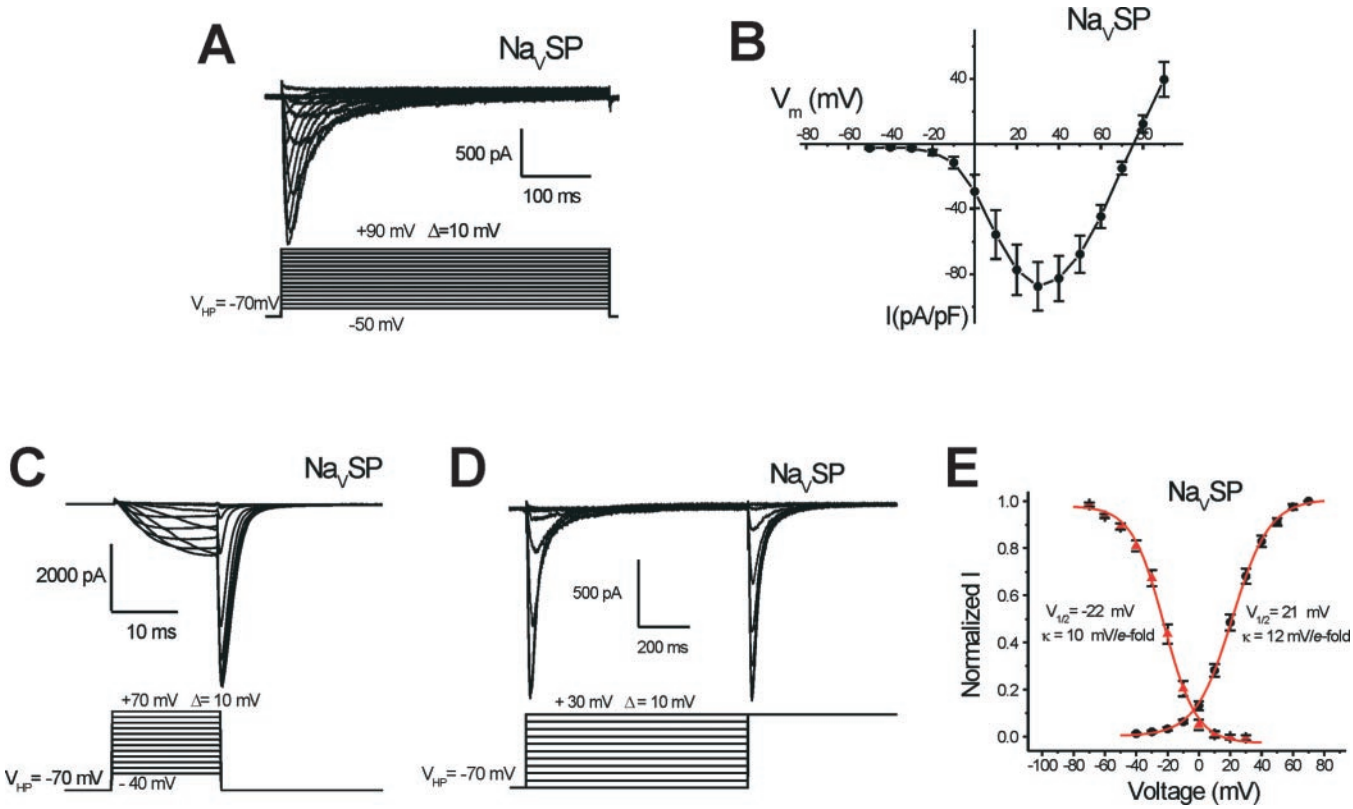

FIG. 5. **Na_VSP voltage-dependent inward currents.** *A*, representative traces (*top*) of I_{Na_VSP} in Tyrode's solution (external) and standard pipette solution. *B*, averaged peak *I*/V relation (n = 23; ±S.E.). I_{Na_VSP} activated above −20 mV and peaked at +30 mV. E_{rev} = +76 mV. *C*, I_{Na_VSP} activation currents. Tail currents were measured as described in the legend to Fig. 4*A*. *D*, I_{Na_VSP} steady-state inactivation currents in response to a protocol similar to that of Fig. 4*B*. *E*, normalized activation curve (n = 28; ±S.E.) and steady-state inactivation curve (n = 11; ±S.E.).

by subthreshold gating of fast Na_V channels (36) or perhaps by $Na_V1.8$ and $Na_V1.9$.

NaChBac selectivity is converted from Na^+ to Ca^{2+} by replacing an amino acid adjacent to glutamatic acid in the putative pore domain by a negatively charged aspartate (from TLESWAS to TLEDWAS or TLDDWAD) (24). Interestingly, two bacterial strains (*C. psychrerythraea* and *M. degradans*) have a putative pore sequence (TFEDWTD) similar to that of the Ca^{2+}-selective NaChBac mutant. We have not been able to functionally express these channel subunits in mammalian cells, but one possibility is that these proteins form heteromeric channels with other related subunits in the same species.

Acknowledgments—We are grateful for bacteria provided by Drs. Hideto Takami, Arthur. A. Guffanti, Terry. A. Krulwich (*O. iheyensis* HTE831), and James D. Oliver (*V. vulnificus* M06) and genomic DNA from Dr. Barbara Methe (*C. psychrerythraea* 34H). We also thank the members of the Clapham laboratory, Nat Blair, and Dr. Terry Krulwich (Mt. Sinai School of Medicine) for valuable comments and encouragement.

REFERENCES

1. Hille, B. (2001) *Ion Channels of Excitable Membranes*, Sinauer, Sunderland, MA
2. Asai, Y., Yakushi, T., Kawagishi, I. & Homma, M. (2003) *J. Mol. Biol.* **327,** 453–463
3. Kojima, S., Yamamoto, K., Kawagishi, I. & Homma, M. (1999) *J. Bacteriol.* **181,** 1927–1930
4. Krulwich, T. A., Ito, M. & Guffanti, A. A. (2001) *Biochim. Biophys. Acta* **1505,** 158–168
5. McCarter, L. L. (2001) *Microbiol. Mol. Biol. Rev.* **65,** 445–462
6. Yorimitsu, T. & Homma, M. (2001) *Biochim. Biophys. Acta* **1505,** 82–93
7. Ren, D., Navarro, B., Xu, H., Yue, L., Shi, Q. & Clapham, D. E. (2001) *Science* **294,** 2372–2375
8. Catterall, W. A. (2000) *Neuron* **26,** 13–25
9. Goldin, A. L., Barchi, R. L., Caldwell, J. H., Hofmann, F., Howe, J. R., Hunter, J. C., Kallen, R. G., Mandel, G., Meisler, M. H., Netter, Y. B., Noda, M., Tamkun, M. M., Waxman, S. G., Wood, J. N. & Catterall, W. A. (2000) *Neuron* **28,** 365–368
10. Catterall, W. A. (2001) *Science* **294,** 2306–2308
11. Sun, Y. M., Favre, I., Schild, L. & Moczydlowski, E. (1997) *J. Gen. Physiol.* **110,** 693–715
12. Yamagishi, T., Li, R. A., Hsu, K., Marban, E. & Tomaselli, G. F. (2001) *J. Gen. Physiol.* **118,** 171–182
13. Ausubel, F. M., Brent, R., Kingston, R. E., Moore, D. D., Seidman, J. G., Smith, J. A. & Struhl, K. (1995) *Current Protocols in Molecular Biology*, Vol. 1, p. 24, John Wiley & Sons, Inc., New York
14. Strom, M. S. & Paranjpye, R. N. (2000) *Microbes Infect.* **2,** 177–188
15. Gonzalez, J. M. & Weiner, R. M. (2000) *Int. J. Syst. Evol. Microbiol.* **50,** 831–834
16. Junge, K., Eicken, H. & Deming, J. W. (2003) *Appl. Environ. Microbiol.* **69,** 4282–4284
17. Meldrum, F. C., Mann, S., Heywood, B. R., Frankel, R. B. & Bazylinski, D. A. (1993) *Proc. R. Soc. Lond. B* **251,** 231–236
18. Gonzalez, J. M., Covert, J. S., Whitman, W. B., Henriksen, J. R., Mayer, F., Scharf, B., Schmitt, R., Buchan, A., Fuhrman, J. A., Kiene, R. P. & Moran, M. A. (2003) *Int. J. Syst. Evol. Microbiol.* **53,** 1261–1269
19. Berry, A., Janssens, D., Humbelin, M., Jore, J. P., Hoste, B., Cleenwerck, I., Vancanneyt, M., Bretzel, W., Mayer, A. F., Lopez-Ulibarri, R., Shanmugam, B., Swings, J. & Pasamontes, L. (2003) *Int. J. Syst. Evol. Microbiol.* **53,** 231–238
20. Moore, R. L., Weiner, R. M. & Gebers, R. (1984) *Int. J. Syst. Bacteriol.* **34,** 71–73
21. McCarthy, A. J. & Cross, T. (1984) *J. Gen. Microbiol.* **130,** 5–25
22. Lu, J., Nogi, Y. & Takami, H. (2001) *FEMS Microbiol. Lett.* **205,** 291–297
23. Takami, H. & Horikoshi, K. (2000) *Extremophiles* **4,** 99–108
24. Yue, L., Navarro, B., Ren, D., Ramos, A. & Clapham, D. E. (2002) *J. Gen. Physiol.* **120,** 845–853
25. Yellen, G. (2002) *Nature* **419,** 35–42
26. Vassilev, P. M., Scheuer, T. & Catterall, W. A. (1988) *Science* **241,** 1658–1661
27. Liu, J., Zhang, M., Jiang, M. & Tseng, G. N. (2002) *J. Gen. Physiol.* **120,** 723–737
28. Imae, Y. & Atsumi, T. (1989) *J. Bioenerg. Biomembr.* **21,** 705–716
29. Krulwich, T. A., Ito, M., Gilmour, R., Sturr, M. G., Guffanti, A. A. & Hicks, D. B. (1996) *Biochim. Biophys. Acta* **1275,** 21–26
30. Hirota, N. & Imae, Y. (1983) *J. Biol. Chem.* **258,** 10577–10581
31. Sugiyama, S., Matsukura, H. & Imae, Y. (1985) *FEBS Lett.* **182,** 265–268
32. Imae, Y., Matsukura, H. & Kobayashi, S. (1986) *Methods Enzymol.* **125,** 582–592
33. Booth, I. R., Edwards, M. D. & Miller, S. (2003) *Biochemistry* **42,** 10045–10053
34. Akopian, A. N., Sivilotti, L. & Wood, J. N. (1996) *Nature* **379,** 257–262
35. Do, M. T. & Bean, B. P. (2003) *Neuron* **39,** 109–120
36. Taddese, A. & Bean, B. P. (2002) *Neuron* **33,** 587–600
37. Perriere, G. & Gouy, M. (1996) *Biochimie* **78,** 364–369